

## Production of C60 plasma

著者	飯塚 哲
journal or publication title	Physics of plasmas
volume	1
number	10
page range	3480-3484
year	1994
URL	<a href="http://hdl.handle.net/10097/35400">http://hdl.handle.net/10097/35400</a>

doi: 10.1063/1.870495

# Production of C<sub>60</sub> plasma

N. Sato, T. Mieno,<sup>a)</sup> T. Hirata, Y. Yagi, R. Hatakeyama, and S. Iizuka  
*Department of Electronic Engineering, Tohoku University, Sendai 980, Japan*

(Received 22 February 1994; accepted 21 June 1994)

An ultrafine-particle plasma consisting of electrons, positive K<sup>+</sup> ions, and large negative C<sub>60</sub><sup>-</sup> ions is produced by introducing "Buckminsterfullerene, C<sub>60</sub>" particles into a low-temperature ( $\approx 0.2$  eV) potassium plasma column confined by a strong axial magnetic field. With an increase in the C<sub>60</sub> fraction, the electron shielding decreases, yielding clear effects on plasma collective phenomena, which are demonstrated for low-frequency electrostatic plasma-wave propagations and instabilities. This plasma might be useful for producing new C<sub>60</sub>-based materials.

## I. INTRODUCTION

Plasmas including dusts or fine particles are of current interest in various fields of physics and engineering.<sup>1</sup> Under the condition of no direct electron-impact ionization and decomposition, large particles are negatively charged up in plasmas such that there is no net electric current to the particles. Even in case of ultrafine particles, if they are electronegative, i.e., their electron affinity is large, they are negatively charged up in plasmas. In most cases, however, fine particles do not have well-defined mass and size, and thus it is often quite difficult to understand plasmas including such dusts or fine particles.

In this work, "Buckminsterfullerene, C<sub>60</sub>" particles<sup>2</sup> are used for the purpose of producing a simple plasma including negative ions; C<sub>60</sub> particles are large cage-like molecules composed of 60 carbon atoms. They are stable, having well-defined mass of mass number  $\approx 720$  and size of about 0.7 nm in diameter. In our work, C<sub>60</sub> particles are introduced into a low-temperature ( $\approx 0.2$  eV) plasma column consisting of electrons and potassium K<sup>+</sup> ions, which is produced by contact ionization of K atoms and is confined radially by a strong axial magnetic field in a Q machine.<sup>3</sup> According to careful analysis of ion species, the plasma obtained consists of electrons, K<sup>+</sup> ions, and C<sub>60</sub><sup>-</sup> ions; C<sub>60</sub> particles are much smaller than usual fine particles but is much larger than positive ions in our plasma. Preliminary measurements of this ultrafine-particle plasma have been reported at the meetings on plasma physics. Some of them will also appear in Ref. 4.

As is well known, since a simple method was established for producing C<sub>60</sub> particles in large quantities,<sup>5</sup> a number of works have been carried out to produce new materials composed of C<sub>60</sub>.<sup>6,7</sup> Our ultrafine-particle plasma might provide a new approach in the field of such a material science.

In Sec. II, experimental apparatus and methods are described. Experimental results are presented, together with discussions, in Sec. III. Section IV contains conclusions.

<sup>a)</sup>Present address: Department of Physics, Shizuoka University, Shizuoka 422, Japan.

## II. EXPERIMENTAL APPARATUS AND METHODS

The experiment is carried out in a single-ended Q machine<sup>3,8</sup> with a vacuum chamber, 15.7 cm in diameter and 400 cm long, with pumping systems at both ends. A plasma consisting of electrons and potassium ions K<sup>+</sup> is produced by contact ionization of K atoms at a hot 5.2 cm diameter tungsten plate heated up to 2000 °C under the "electron-rich" condition. The background gas pressure is smaller than  $1 \times 10^{-6}$  Torr. The plasma column, with density  $n_p = (1.0 \sim 5.0) \times 10^9$  cm<sup>-3</sup> and electron temperature  $T_e \approx 0.2$  eV  $\geq T_+$  (ion temperature), flows along a uniform magnetic field  $B \leq 4$  kG and is terminated by a metal endplate situated at a distance of 210 cm from the hot plate, which is kept at floating potential.

As shown schematically in Fig. 1, a Q-machine plasma passes through a copper cylinder of 7.6 cm in diameter and 20 cm long, situated at a position around the machine center. The cylinder has a 3 cm diameter hole on the side wall, where we set an oven for sublimation of C<sub>60</sub>. The oven, which is also made of copper, has a small hole to inject C<sub>60</sub> in the direction toward the Q-machine plasma. The fullerene C<sub>60</sub>, which is produced by discharge between carbon electrodes in a closed system,<sup>5,9</sup> is kept as a soft film on the inner surface of the oven. The temperature for the C<sub>60</sub> sublimation is in the range 350~400 °C. The oven temperature  $T_0$ , measured at its bottom, is carefully changed to cover this temperature range while the cylinder is kept at a constant temperature around 400 °C. In the region surrounded by the cylinder, the density of C<sub>60</sub> particles sublimated is in the range  $\leq 10^{13}$  cm<sup>-3</sup>, depending on  $T_0$ , which corresponds to the pressure range  $\leq 10^{-6}$  Torr. These values are estimated from a C<sub>60</sub> decrease in the oven. In the region outside the cylinder, the density and pressure of C<sub>60</sub> particles are smaller by one to two orders of magnitude than those inside the cylinder.

Most of plasma parameters are measured by movable Langmuir probes with heating systems to keep their surfaces clean. An "omegatron" analyzer<sup>10</sup> also with heating system, situated behind a small hole of the endplate, is used for analyzing ion species. This analyzer yields signals due to the cyclotron resonances of ion species. There appear peaks in a collector current  $I_c$  of the analyzer when a frequency of ap-

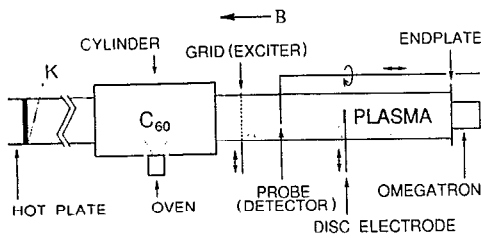


FIG. 1. Experimental apparatus.

plied radio frequency (RF) electric field is equal to the ion cyclotron frequencies. It is also possible to identify the ion species by measuring low-frequency electrostatic plasma-wave propagations and instabilities.<sup>11</sup>

### III. EXPERIMENTAL RESULTS AND DISCUSSIONS

The  $C_{60}$  control is monitored by measuring a negative-saturation current of the Langmuir probe,  $I_{s-}$ , which depends on  $T_0$ . A typical variation of  $I_{s-}$  is demonstrated in Fig. 2, where the probe is set at the radial center. With an increase in  $T_0$ ,  $I_{s-}$  decreases, implying a decrease in electron density  $n_e$  because a change in  $T_e$  is not observed. In this experiment, the electron fraction  $1-\epsilon$  is found to decrease to the value around  $1 \times 10^{-1}$  at the radial center, where  $\epsilon = n_- / n_p$  ( $n_p = n_+ \approx n_e + n_-$  if  $Z=1$ ) with positive and negative ion densities,  $n_+$  and  $n_-$ , respectively. This value is not as small as in case of  $SF_6$ -gas introduction into a Q-machine plasma.<sup>11-13</sup> This is partly because the electron affinity ( $\approx 2.65$  eV) is smaller than that of  $SF_6$  ( $\approx 3.39$  eV). But, we must be careful about a radial plasma structure modified in the presence of  $C_{60}^-$  ions, the Larmor radius ( $\approx 0.46$  cm at  $B=2$  kG) of which is much larger than that of  $K^+$  ions.

Figure 3 shows typical probe characteristics, i.e., probe current  $I_p$  against potential difference  $V_p$  applied between the probe and the hot plate which is electrically grounded together with the vacuum chamber (the cylinder and the oven are kept floating), at radial positions (a)  $r=0$  cm and (b)  $r=1.5$  cm. It can be found in Fig. 3(a) that there also appears a decrease in the positive-saturation current  $I_{s+}$  in addition to a decrease in  $I_{s-}$  when  $T_0$  is increased. But,  $I_{s-}$  decreases

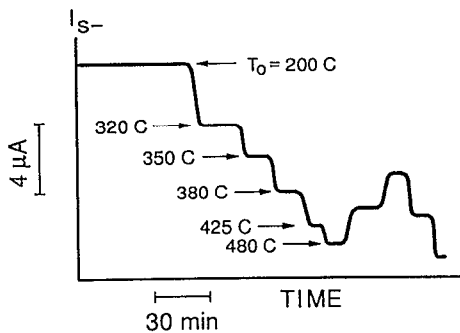


FIG. 2. Control of  $C_{60}$  particles: negative probe-saturation current  $I_{s-}$  against  $T_0$ .

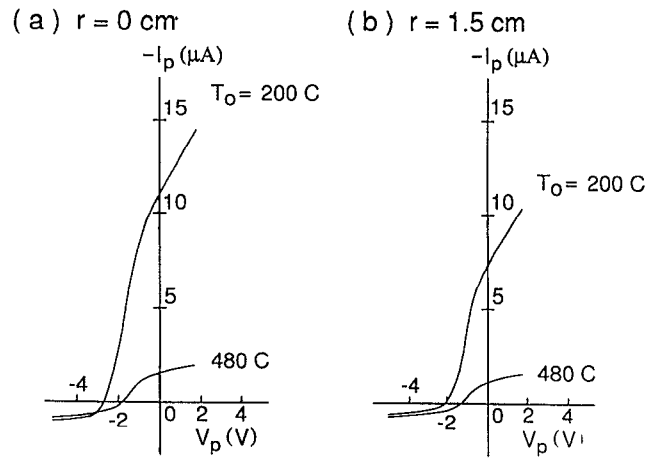


FIG. 3. Typical probe characteristics at (a)  $r=0$  cm and (b)  $r=1.5$  cm with  $T_0$  as a parameter.  $B=2.0$  kG.

more drastically than  $I_{s+}$ . This means that the decrease in  $n_e$  is accompanied by an increase in  $n_-$ . On the other hand, however, at  $r=1.5$  cm, with an increase in  $T_0$ ,  $I_{s+}$  increases while  $I_{s-}$  decreases, as shown in Fig. 3(b). The increase in  $I_{s+}$  implies an increase in  $n_p (=n_+)$  at this position. Here it is to be noted that neither plasma cooling nor heating due to the  $C_{60}$  introduction can be supposed in our pressure range of  $C_{60}$ .

An effect of  $C_{60}$  particles on the radial plasma profile is presented in Fig. 4. Since  $n_p (=n_+)$  is proportional to  $I_{s+}$ , the  $I_{s+}$  profile corresponds to a radial variation of the plasma density. On the other hand,  $I_{s-}$  includes currents due to electrons and negative ions. The ratio of electron to negative-ion current is given by  $(n_e/n_-)(T_e m_- / T_- m_e)^{1/2}$  for electrons of

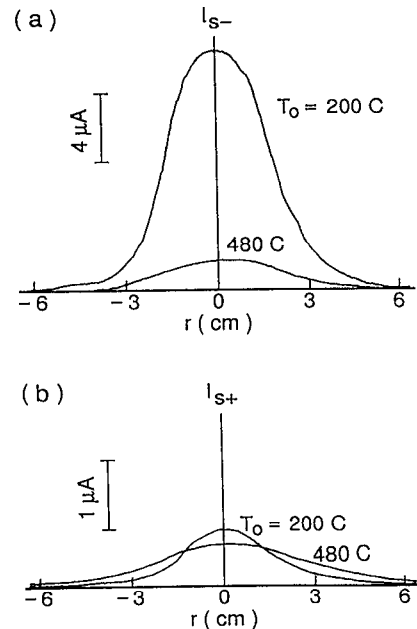


FIG. 4. Radial profiles of (a)  $I_{s-}$  and (b)  $I_{s+}$  with  $T_0$  as a parameter.  $I_{s-}$  and  $I_{s+}$  are negative and positive probe-saturation currents, respectively.  $B=2.0$  kG.

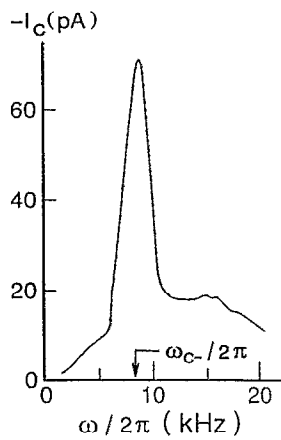


FIG. 5. Collector current  $I_c$  of the omegatron as a function of frequency  $\omega/2\pi$  of applied RF field at  $B=3.85$  kG and  $T_0=480$  °C.

mass  $m_e$  and temperature  $T_e$  and negative ions of mass  $m_-$  and temperature  $T_-$ . Since this ratio is  $1.9 \times 10^3 (n_e/n_-)$  in our case, the negative-ion current is larger than the electron current only when  $n_e/n_- \leq 5.0 \times 10^{-4}$  is satisfied, where  $T_-$  is assumed to be 0.07 eV because  $T_0 \leq 500$  °C. In this experiment, the electron current is much larger than the negative-ion current. Thus the  $I_{s-}$  profile gives a radial variation of  $n_e$  even in the presence of  $C_{60}$  particles. As shown in Fig. 4, in the absence of  $C_{60}$  particles ( $T_0=200$  °C), the  $I_{s-}$  profile is almost the same as the  $I_{s+}$  profile. By introducing  $C_{60}$  particles, the  $I_{s+}$  profile becomes broad, showing a plasma spread in the radial direction. This is due to the large Larmor radius of negative  $C_{60}$  ions. The  $I_{s-}$  profile becomes also broad but is not as broad as the  $I_{s+}$  profile, implying that electrons are rather well confined by the magnetic field. Thus, the fraction of negative  $C_{60}$  ions increases, i.e.,  $1-\epsilon$  decreases, resulting in a formation of local plasma structure, in the radial direction. In case of the measurements shown in Fig. 4, we obtain  $1-\epsilon=0.2$  in the central region ( $r \leq 1.5$  cm) but  $1-\epsilon=0.1$  at  $r=3.0$  cm, being followed by a further decrease in the plasma edge region.

In order to know how many electrons are attached to the  $C_{60}$  particle, ion species are analyzed by using the omegatron analyzer.<sup>10</sup> The collector current of the analyzer,  $I_c$ , is plotted as a function of frequency  $\omega/2\pi$  of applied RF electric field for cyclotron acceleration. A typical example of the spectra measured is shown in Fig. 5. A clear peak of  $-I_c$  is found in addition to the positive peak due to  $K^+$  ions at  $\omega_{c+} (=eB/m_+)/2\pi$ . A dependence of the frequency giving this negative peak on  $B$  is presented in Fig. 6. The results show a good agreement with predicted values of  $\omega_{c-} (=eB/m_-)/2\pi$  for  $C_{60}^-$  ions. Thus, we can conclude that our negative  $C_{60}$  ions are exactly  $C_{60}^-$ .

A decrease in  $n_e$  gives rise to a decrease in the electron shielding for potential variations. As a result, there appear changes of plasma collective phenomena, which are clearly observed for low-frequency electrostatic plasma-wave propagations and instabilities.<sup>11</sup>

Ion waves are typical low-frequency electrostatic plasma waves. In the presence of negative ions, there are two

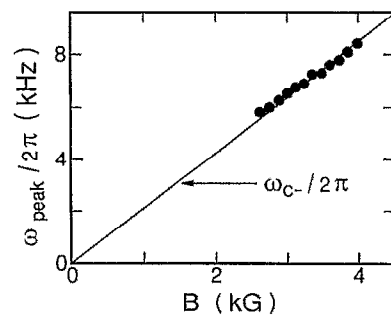


FIG. 6. Frequency at the negative peak in the omegatron spectrum (see Fig. 5),  $\omega_{\text{peak}}/2\pi$ , as a function of  $B$  at  $T_0=480$  °C. The solid line indicates the predicted cyclotron frequency of  $C_{60}^-$ .

branches of propagation, i.e., fast and slow modes, corresponding to two ion species.<sup>11,14,15</sup> In our experiment, a grid is used to generate ion waves propagating along a magnetic field toward the downstream region.<sup>8</sup> Small sinusoidal potential variations within 0.1 V peak-to-peak are applied to the grid which is biased a little positively with respect to the floating potential. Typical wave patterns obtained from an interferometer detection system are demonstrated in Fig. 7. It can be found in Fig. 7(b) that there are two modes in the presence of negative  $C_{60}$  ions. One of them, the mode with long wavelength (fast mode), propagates even in the absence of  $C_{60}^-$  ions, as shown in Fig. 7(a). This mode is due to  $K^+$  ions. The mode with short wavelength (slow mode) propagates only when there are  $C_{60}^-$  ions. Figure 8 presents dispersion relations of these two modes, which yield linear relations between  $\omega/2\pi$  and  $k$  (wave number). This means that the both modes corresponds to ion sound waves with phase velocities  $v_p (= \omega/k)$  independent of  $\omega/2\pi$ .

In a plasma consisting of electrons, positive ions, and negative ions, the phase velocities of the fast and slow modes are given by  $(\omega/k)^2 = [T_e/(1-\epsilon) + 3T_+]/m_+$  and  $(\omega/k)^2 = [\epsilon T_e/(1-\epsilon + T_e/T_+) + 3T_-]/m_-$ , respectively, where  $m_- \gg m_+$  and  $T_e \gg T_+ > T_-$  are assumed. In the experiment,  $T_e \gg T_+ > T_-$  and there is a flow of  $K^+$  ions, which is due to acceleration by the electron sheath of potential drop  $\geq 0.5$  V in front of the hot plate. Thus the above expressions cannot be directly applied to our experiment. But, a qualita-

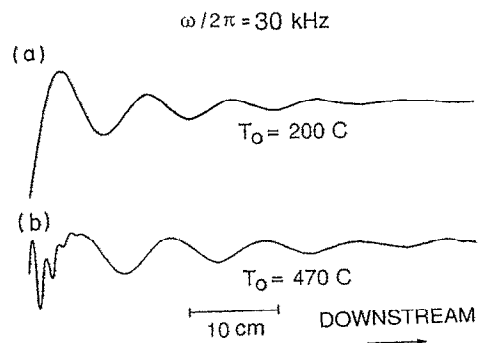


FIG. 7. Wave patterns of ion waves with frequency  $\omega/2\pi=30$  kHz at (a)  $T_0=200$  °C and (b)  $T_0=470$  °C.

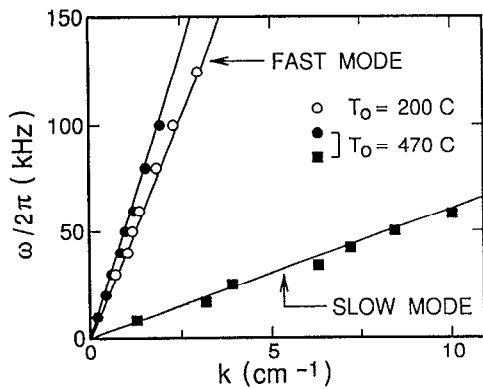


FIG. 8. Dispersion relations of fast and slow ion waves at  $T_0=200\text{ }^\circ\text{C}$  and  $470\text{ }^\circ\text{C}$ . The best fit lines (straight solid lines) yield the phase velocities  $v_p=2.5\times 10^5\text{ cm/s}$  (fast mode,  $T_0=200\text{ }^\circ\text{C}$ ),  $3.3\times 10^5\text{ cm/s}$  (fast mode,  $T_0=470\text{ }^\circ\text{C}$ ), and  $3.8\times 10^4\text{ cm/s}$  (slow mode,  $T_0=470\text{ }^\circ\text{C}$ ).

tive behavior of ion sound waves is well described by these relations. With a decrease in  $1-\epsilon$ ,  $v_p$  increases for the both modes, as observed in the experiment. It is also predicted that the fast mode is more sensitive to  $1-\epsilon$  than the slow mode. By measuring  $v_p$  of the fast mode, we can estimate  $1-\epsilon$  even if  $1-\epsilon$  is so small that the probe does not give a correct value of  $1-\epsilon$ .<sup>11</sup>

An example of low-frequency electrostatic instabilities is an ion-cyclotron wave instability.<sup>16</sup> The instability is triggered by applying a positive potential to a small disk electrode situated in front of the endplate. A number of experiments have been performed on this instability,<sup>17</sup> although there are still discussions about the generation mechanism.<sup>18</sup> In the presence of negative ions, there appear two modes of instability<sup>11,13</sup> with frequencies given by  $\omega^2 \approx \omega_{c+}^2 + [T_e/m_+(1-\epsilon)]\kappa^2$  and  $\omega^2 \approx \omega_{c-}^2 + [\epsilon T_e/m_- \times (1-\epsilon + \rho_{+s}^2 \kappa^2)]\kappa^2$ , where effects of the finite ion Larmor radius are neglected,  $\kappa$  is the wave number perpendicular to the magnetic field, and  $\rho_{+s}^2 = m_+ T_e / e^2 B^2$ . Both of them have the frequencies higher than  $\omega_{c+}/2\pi$  and  $\omega_{c-}/2\pi$ , respectively. Their separations from  $\omega_{c+}/2\pi$  and  $\omega_{c-}/2\pi$  increase as  $1-\epsilon$  is decreased. Figure 9 shows a typical frequency spectrum observed. When  $C_{60}$  particles are introduced, there appears a signal due to  $C_{60}^-$  ions in addition to the signal due to  $K^+$  ions. The frequency is higher than  $\omega_{c-}/2\pi$ , as found in Fig. 10, and increases with a decrease in  $1-\epsilon$ , as predicted

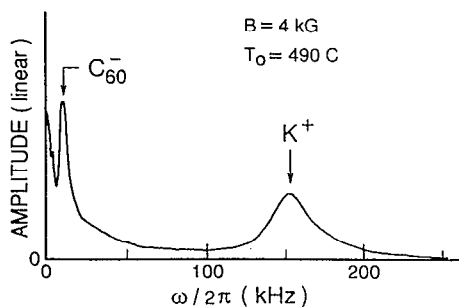


FIG. 9. A typical frequency spectrum of electrostatic ion-cyclotron wave instabilities at  $B=4.0\text{ kG}$  and  $T_0=490\text{ }^\circ\text{C}$ .

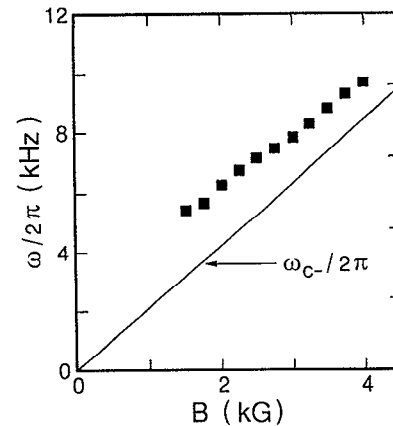


FIG. 10. Frequency  $\omega/2\pi$  of ion-cyclotron wave instability due to  $C_{60}^-$  ions as a function of magnetic field  $B$  at  $T_0=490\text{ }^\circ\text{C}$ .

theoretically, although the flow of  $K^+$  ions and the finite ion Larmor radius have to be taken into account in order to obtain a quantitative agreement between the measured and predicted values.

#### IV. CONCLUSIONS

An ultrafine-particle plasma with  $C_{60}^-$  is produced by introducing  $C_{60}$  particles into a magnetized low-temperature plasma, where there is no electron-impact ionization and decomposition. The  $C_{60}^-$  fraction,  $n_-/n_+$ , is controlled in the range  $\approx 0.9$ . With an increase in  $n_-/n_+$ , the electron shielding effect decreases, yielding clear changes of plasma collective phenomena, as demonstrated for ion-wave propagations and ion-cyclotron wave instabilities.

Because of its simplicity, the plasma produced would be useful for investigating ultrafine-particle plasmas. This plasma might be attractive also in the field of material science. Various knowledges and techniques established in plasma physics and engineering could be applied to control of  $C_{60}$  particles for producing  $C_{60}$ -based materials.

#### ACKNOWLEDGMENT

One of the authors (N.S.) would like to thank Professor H. Ikegami for his useful discussions about  $C_{60}$ -plasma production.

<sup>1</sup>C. K. Goertz, *Rev. Geophys.* **27**, 271 (1989).

<sup>2</sup>H. W. Kroto, J. R. Heath, S. C. O'Brien, R. F. Curl, and R. E. Smalley, *Nature* **318**, 162 (1985).

<sup>3</sup>R. W. Motley, *Q. Machines* (Academic, New York, 1975).

<sup>4</sup>N. Sato, "Production of negative-ion plasmas in a Q machine," *Plasma Sources Sci. Technol.* (in press, 1994).

<sup>5</sup>W. Krätschmer, L. D. Lamb, K. Fortiropoulos, and D. R. Huffman, *Nature* **347**, 354 (1990).

<sup>6</sup>A. F. Hebard, M. J. Rosseinsky, R. C. Haddon, D. W. Murphy, S. H. Glarum, T. T. M. Palstra, A. P. Ramirez, and A. R. Kroton, *Nature* **350**, 600 (1991).

<sup>7</sup>L. P. Hare, H. W. Kroto, and R. Taylor, *Chem. Phys. Lett.* **177**, 394 (1991).

<sup>8</sup>N. Sato, H. Sugai, A. Sasaki, and R. Hatakeyama, *Phys. Rev. Lett.* **30**, 685 (1973).

<sup>9</sup>T. Mieno, H. Takatsuka, E. Kumekawa, A. Sakurai, and T. Asano, *J. Plasma Fusion Sci. Res.* **69**, 793 (1993).

- <sup>10</sup>H. Sommer, H. A. Thomas, and J. A. Hipple, *Phys. Rev.* **82**, 697 (1951).
- <sup>11</sup>N. Sato, *A Variety of Plasmas*, edited by A. Sen and P. K. Kaw (Indian Academy of Sciences, Bangalore, 1989), p. 79.
- <sup>12</sup>D. R. Sheehan and N. Rynn, *Rev. Sci. Instrum.* **59**, 1661 (1988).
- <sup>13</sup>B. Song, B. Suszcynsky, N. D'Angelo, and R. L. Merlino, *Phys. Fluids B* **1**, 2316 (1989).
- <sup>14</sup>N. D'Angelo, S. V. Goeler, and T. Ohe, *Phys. Fluids* **9**, 1605 (1966).
- <sup>15</sup>B. Song, N. D'Angelo, and R. L. Merlino, *Phys. Fluids B* **3**, 284 (1991).
- <sup>16</sup>N. D'Angelo and R. W. Motley, *Phys. Fluids* **5**, 663 (1962).
- <sup>17</sup>J. J. Rasmussen and R. Schrittwieser, *IEEE Trans. Plasma Sci.* **PS-19**, 457 (1991).
- <sup>18</sup>N. Sato and R. Hatakeyama, *J. Phys. Soc. Jpn.* **54**, 1661 (1985).